Performance Optimization of Vertical Nanowire-based Piezoelectric Nanogenerators

Ronan Hinchet, Sangmin Lee, Gustavo Ardila, Laurent Montès, Mireille Mouis, and Zhong Lin Wang**

The integrated nanogenerator (NG) based on vertical nanowire (NW) arrays is one of the dominant designs developed to harvest mechanical energy using piezoelectric nanostructures. Finite element method (FEM) simulations of such a NG are developed using ZnO NWs in compression mode to evaluate its performances in term of piezoelectric potential generated, capacitance, induced mechanical energy, output electrical energy, and efficiency. This evaluation is essential to correctly understand NG operation. Three main issues are highlighted. The mechanical and electrical structures of the NG as an integrated system are optimized, and strategies for concentrating the mechanical strain field in the NWs and increasing the force sensitivity are developed. In addition, the influence of NWs length and diameter on NG performances is investigated. The optimization results in a piezoelectric nano composite material where global performances are improved by mean of long and thin NWs.

1. Introduction

Harvesting green and renewable energy from environment is one effective response to the actual energy crisis and to the power supply of nano- and microdevices. Mechanical energy[1] is among the most abundant and reliable energy sources in our daily life, regardless of weather or temperature conditions, in contrast with solar[2] and thermoelectric energies.[3] New materials, structures and technologies have been subjects of active research and development.[4–7] Likewise, at the nanoscale, energy harvesting nanotechnologies based on the piezoelectric effect have been developed to harvest small-scale and irregular sources of mechanical energy present in our living environment, such as air flow[8] or heart beating,[9] among others. Moreover, due to their small size, energy harvesting devices can be effectively integrated with other nano/micro scale functional devices to build self-powered systems.[10] Thus, over the past few years, semiconductor piezoelectric nanowires (piezo NWs) have been extensively investigated as the building blocks of piezoelectric mechanical energy harvesters called nanogenerators (NG)[11–13] as well as for sensors.[12,14–17] The fundamental operation mechanism of a NG relies on the piezoelectric potential (piezo potential) generated in NWs when strained by an external force. The use of nanostructures has been firstly motivated by their improved piezoelectric properties.[18,19] Nanostructured materials like ZnO, GaN,[20,21] PZT,[22,23] $BaTiO_3$,[24,25] $NaNbO_3$,[26] and PVDF[27] as nanowires, nanobeams or nanopillars have been used. Among them, ZnO is lead free, biocompatible and it can be grown easily in NWs at low temperature (85 °C) on several substrates. Moreover, it can even be exploited for solar, thermal and mechanical hybrid energy harvester.[28] In recent years, the NG design has evolved with lateral,[29–32] radial,[33,34] and vertical[31,35] integrated nanowires. Improvements in the integration[36,37] and new strategies have been proposed[11,31,35,38] to cancel or decrease the effects of disturbing phenomena that occur in semiconducting NWs, such as piezo potential screening by free carriers.[39–42] However, this is not the only issue. The full potential of nanostructures has still not been fully exploited in NG whereas it can provide new advantages such as higher force sensitivity, higher surface/volume ratio and better quality of the materials. To this end, mechanical and electrical characteristics of NG structures need to be evaluated and optimized.

The vertical integrated NG (VING) structure, is the dominant design used to harvest compressive and bending mechanical energy.[43] Compared to lateral and radial structures, the fabrication and integration of VING is far easier. Few lift-off fabrication steps are required and a large surface can be functionalized and integrated on selective areas.[42] The VING stacked structure is convenient to add and tune different layers between the NWs. Moreover, this device is rather robust because of its bulk structure. It can work in compression mode and, with a lower yield, in bending modes.[44] In this paper, however, we will only consider the compression mode.

In this paper, the VING structure was studied based on computer simulation. Using finite element method (FEM)

R. Hinchet, Dr. G. Ardila, Dr. L. Montès, Dr. M. Mouis
IMEP-LAHC, MINATEC
3 rue Parvis Louis Neel, 38016, Grenoble, France
E-mail: ardilarg@minatec.inpg.fr
Dr. S. Lee, Prof. Z. L. Wang
School of Materials Science and Engineering
Georgia Institute of Technology
Atlanta, Georgia, 30332–0245, USA
Prof. Z. L. Wang
Beijing Institute of Nanoenergy and Nanosystems
Chinese Academy of Sciences, Beijing, China
E-mail: zlwang@gatech.edu

DOI: 10.1002/adfm.201302157

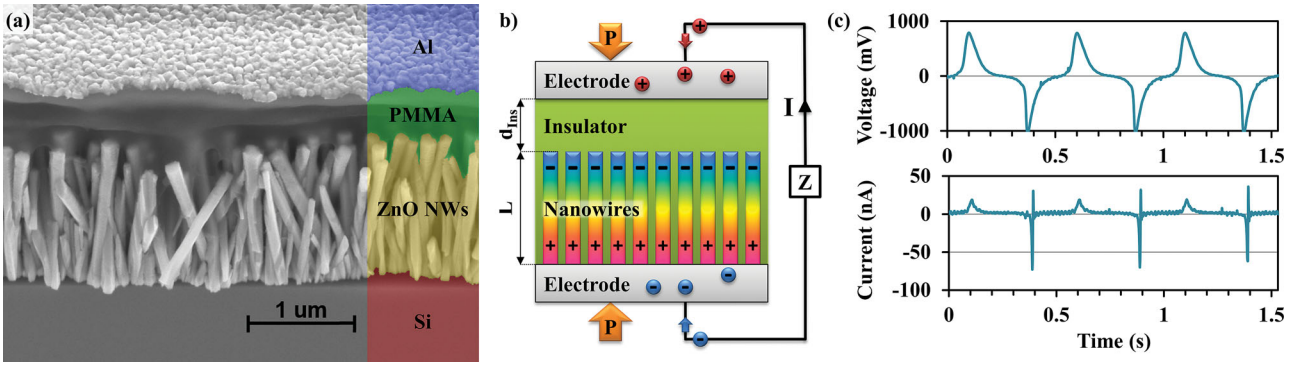

Figure 1. a) SEM image, tilted cut view of a VING prototype using ZnO NWs, b) Schematics of the VING structure working as a charged capacitance proportional to the force applied, c) Voltage and current characterization of a VING prototype under AC compression.

simulations, we evaluated the influence of VING structural parameters on such figures of merit as generated piezoelectric potential, capacitance, induced mechanical energy, output electrical energy and efficiency. This evaluation is essential to fully understand the operation of the NG. Three main issues were highlighted: the strain distribution around the NWs, the dielectric losses in the insulating layer and piezo potential screening by free carriers. We optimized the mechanical and electrical structure of the VING, concentrating the mechanical strain field in the NWs and increasing the force sensitivity. In addition, we investigated the influence of NWs length and diameter on NG performances. The optimization resulted in a piezoelectric composite material where global performances were improved by mean of long and thin NWs.

2. Results and Discussion

The VING structure inspired from[31] was considered as the simplest design developed to build NGs using piezo NWs (**Figure 1**a). This harvester can be divided into 3 parts (Figure 1b). First, a piezo NW array converts mechanical energy into electrical energy via piezoelectric effect. This is the core of the device. In the following simulations we considered undoped ZnO NWs to study the electromechanical structure of the NG, but this approach could be transferred to other materials such as GaN and AlN NWs. Secondly this matrix of NWs is immerged into an insulating layer which increases mechanical robustness and protects it from the electrical leakages and short circuits that could occur because of the n-type non intentional doping concentration[36,45] of the as grown ZnO NW. In this study we used PMMA as interstitial material. Finally, top and bottom electrodes are used to collect electrical charges. In practice, the substrate can be readily used as the bottom electrode. The working principle is the following (Figure 1b): the mechanical forces and the impacts compress the piezo NWs along their *c*-axis, thus generating a voltage difference across them due to the piezoelectric effect, which drives electrons to flow across the external circuit in order to compensate this potential difference. The voltage generated by the compressed NWs drives charges from the external circuit and accumulates them at the top and bottom electrodes, charging the capacitance and generating a current pulse. An opposite displacement current is generated when the force is released (Figure 1c).

The electrical potential generated by strain has already been investigated for individual piezo NWs.[18] Here, to go further, we performed FEM simulation of the full NG structure using COMSOL Multiphysics software.[46] We considered small deformations, anisotropic materials and no free charges in the nanowire. We solved the linear mechanical Equation 1 that links the stress T to the applied force F on the NG and the Poisson Equation 2 that links the electric displacement D to the fixed charge density ρ_v.

$$-\nabla \cdot T = F \tag{1}$$

$$\nabla \cdot D = \rho_V \tag{2}$$

These equations were coupled by the piezoelectric Equations (3,4) that correlate the stress T tensor, the strain S, the electric displacement D, and the electric field E using the permittivity ε, the elasticity tensor c and the piezoelectric coupling tensor e. We remained in the linear approximation limit with linear tensors c and e. Indices p, q, I, and k refers to the indices of the coefficient matrix and the exponent t refer to the transpose of the matrix.

$$T_p = c_{pq} \cdot S_q - e^t_{kp} \cdot E_k \tag{3}$$

$$D_i = e_{iq} \cdot S_q - \varepsilon_{ik} \cdot E_k \tag{4}$$

The simulated structure was an array of NG elementary cells (**Figure 2**a) surrounded by air. The elementary cell structure consists of one ZnO NW immerged in a PMMA medium with top and bottom electrodes. The reference cell includes a NW with radius (r) of 25 nm and length (L) of 600 nm, cell size is 100 nm × 100 nm × 700 nm, the thickness of the PMMA layer above the NWs (d_{ins}) is 100 nm. As boundary conditions we applied a ground and fixed constraint condition to the bottom electrode. The normal displacement of the core cell sidewalls was set to zero using symmetry conditions. The top electrode of the NG core cell was rigid with floating potential. Finally a pressure of 1 MPa was applied on the top of the cell. While the behavior of piezo NWs under compression is well understood[47] a wide range of values is observed in the literature

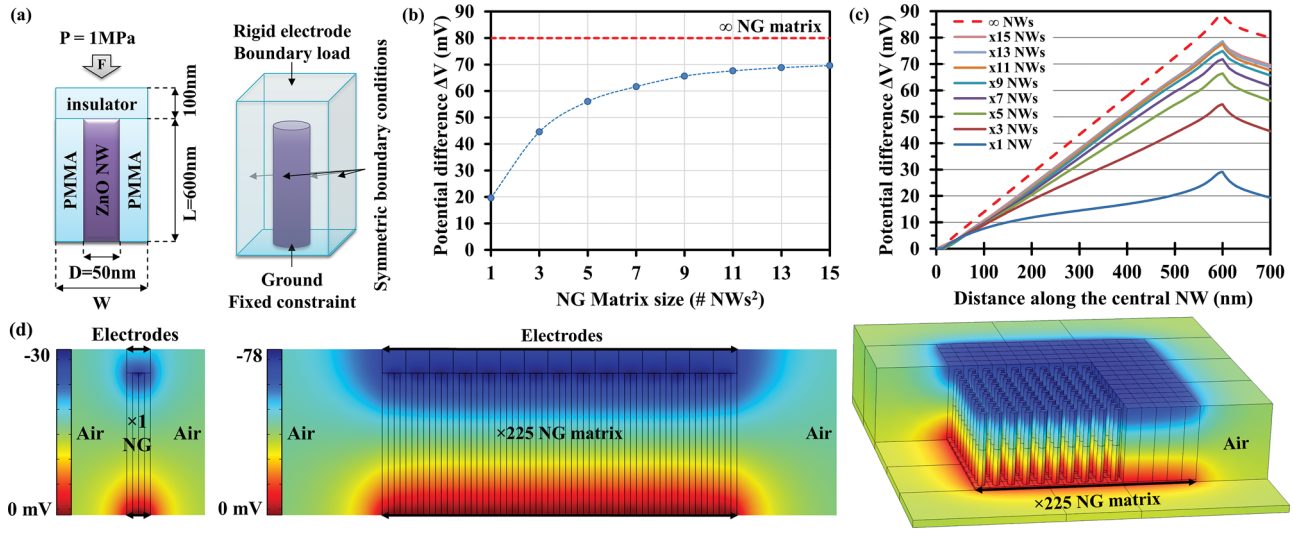

Figure 2. a) Schematics of the geometry and boundary conditions used to perform FEM simulations on a NG core cell. b) Evolution of the difference of electric potential generated at the top electrode by a NG surrounded by air as a function of the NG matrix size. c) Evolution of the electric potential generated through the central NW of various NG matrix sizes surrounded by air as a function of the distance from the NWs root at the bottom. d) FEM simulation of the distribution of the electric potential generated by various NG matrix sizes embedded with PMMA and Si_3N_4, surrounded by air and strained under 1 MPa, as a function of the NG matrix size.

for generating piezo potential.[42] In this study, we considered bulk materials properties, although several studies[18] have shown that electromechanical and piezoelectric properties are enhanced at nanoscale. For a NG core cell, we defined a ratio parameter R as the NW diameter (D) divided by the core cell width (W), representing the NW density. First simulations were performed depending on the matrix size, that is the number of elementary cells in the NG (Figure 2b), which show the influence of the NG surface on its performances.

The electric potential generated between the electrodes increases from 20 mV to 70 mV as the NG matrix size increases from 1 cell × 1 cell to 15 cells × 15 cells, that is up to 225 NWs (Figure 2c), and it converges to a maximum value of 80 mV corresponding to the electric potential generated without taking into account edge effect and dielectric losses (Figure 2b,c). Figure 2d represents the piezo potential distribution for 1 single cell and for a 15 cells × 15 cells matrix, both surrounded by air. The piezo potential generated from one NG cell is low (20 mV) and it shows strong edge effects and 3D dielectric losses that are not representative of a cell behavior in the NG which is embedded into a large array. As the matrix size increases, edge effects and 3D dielectric losses decreases. The piezo potential saturates for a matrix size of around 200 NWs. Therefore, it is necessary to aggregate at least ensembles of 200 NWs to obtain an efficient NG.

In a second step, an extensive parameter screening was carried out based on the simulation of the core cell (Figure 2d) without surrounding air and edge effect. However, we still considered the coupling effect between the piezo NW and the charged top and bottom electrodes. This coupling decreased the generated piezo potential by up to 40% due to the screening effect of the charges accumulated in the electrodes of the device. The first prototype was built, using a high density of ZnO NWs and a thick PMMA insulating layer (d_{ins} = 3 um), presenting low performances. In a recent study on the mechanical optimization of VING devices,[48] we reported an optimized device structure using a thin (d_{ins} = 100 nm) PMMA insulating layer on top of the NWs and a medium density (R = 0.5) of ZnO NWs. Several parameters and materials were investigated. The main issues were the dielectric losses and the non-homogenous structure of the NWs layer. The 3D dielectric losses occurred for low and medium NW density combined with a thick insulating layer, as the non-homogenous structure drives the strain field to flow around the NWs. All these problems were reducing the piezo potential generated and the mechanical and electrical energy stored. In our previous study,[48] we demonstrated that the capacitance and the electrical potential could be improved by using a thinner insulating layer and adapted NW density, which increased electrostatic coupling. Here, we propose a new structure using various materials used in microelectronics such as Al_2O_3, Si_3N_4, or SiO_2 as top insulating layers. We investigated and analyzed the geometry and the materials used to improve the mechanical energy stored, the energy conversion and the electrical energy stored in the NG.

The insulating layer on the VING structure was divided in two parts: (layer 1) the insulator above the NWs and (layer 2) the interstitial insulator between the NWs. We considered the NG analytical models developed previously in[48] and the yield Equations (5) and (6):

$$\eta_{\text{Mechanical energy transfer}} = \frac{1}{1 + \frac{d_1 \cdot E_2}{d_2 \cdot E_1}} \quad (5)$$

$$\eta_{\text{Electrical energy transfer}} = \frac{1}{1 + \frac{d_1 \cdot \varepsilon_2}{d_2 \cdot \varepsilon_1}} \quad (6)$$

where d_x, E_x, and ε_x are respectively the thickness, Young's modulus and permittivity of the layer (x). Here, we propose to use

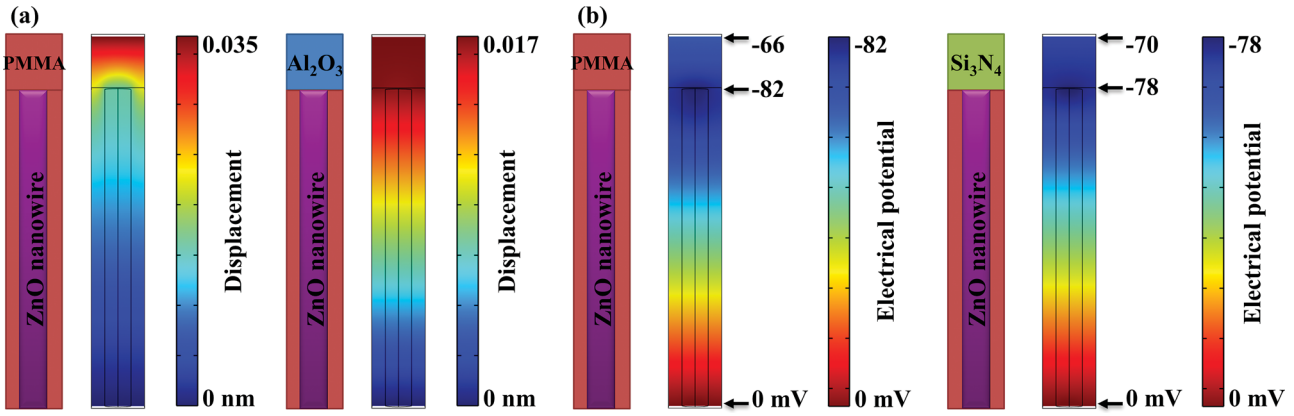

Figure 3. Schematic and FEM simulation of various NG structures. a) Distribution of the displacement in a NG core cell with PMMA or Al_2O_3 as top insulating layer. b) Distribution of the electric potential in a NG core cell with PMMA or Si_3N_4 as top insulating layer.

different materials for the top insulating layer and the interstitial insulating material so that mechanical and electrical energy stored mechanism are dissociated from piezoelectric energy conversion mechanism. This allows each term to be optimized separately. The idea is to target high Young's modulus and permittivity for the top insulator and low Young's modulus and permittivity for the interstitial insulator, in order to maximize the energy stored in the NG. Concretely, to decrease the effect of the non-homogeneous distribution of strain around the NWs we used a hard material like Al_2O_3 (Young's modulus = 400 GPa) as a top insulator. Then to increase the sensitivity of the piezo NWs layer to small forces,[48] we used a softer material such as PMMA as an interstitial insulator. As a result (**Figure 3**a), the deviation of the strain field in the structure significantly decreased and the strain was linearly distributed in the NWs layer, which is closer to the NG analytical model developed in.[48] This structure allows maximizing transmission of external mechanical energy to piezo NWs which are the core of the NG. On the other hand, dielectric losses decreases the electric potential transmission from NWs to top electrode (Figure 3b) leading to a decrease of stored electrical energy. Even if these losses are small and mainly occur for low NW density and thick insulating layer, we can minimize them by using a high permittivity (high-*k*) insulator. Among the insulators studied here, Si_3N_4 featured the best trade-off because of its large Young's modulus (250 GPa) and relatively high permittivity (9.7) (Figure 3b).

To further optimize this new structure, we studied the effect of the NW density on the NG properties (**Figure 4**a). We computed mechanical energy, electrical energy and total efficiency

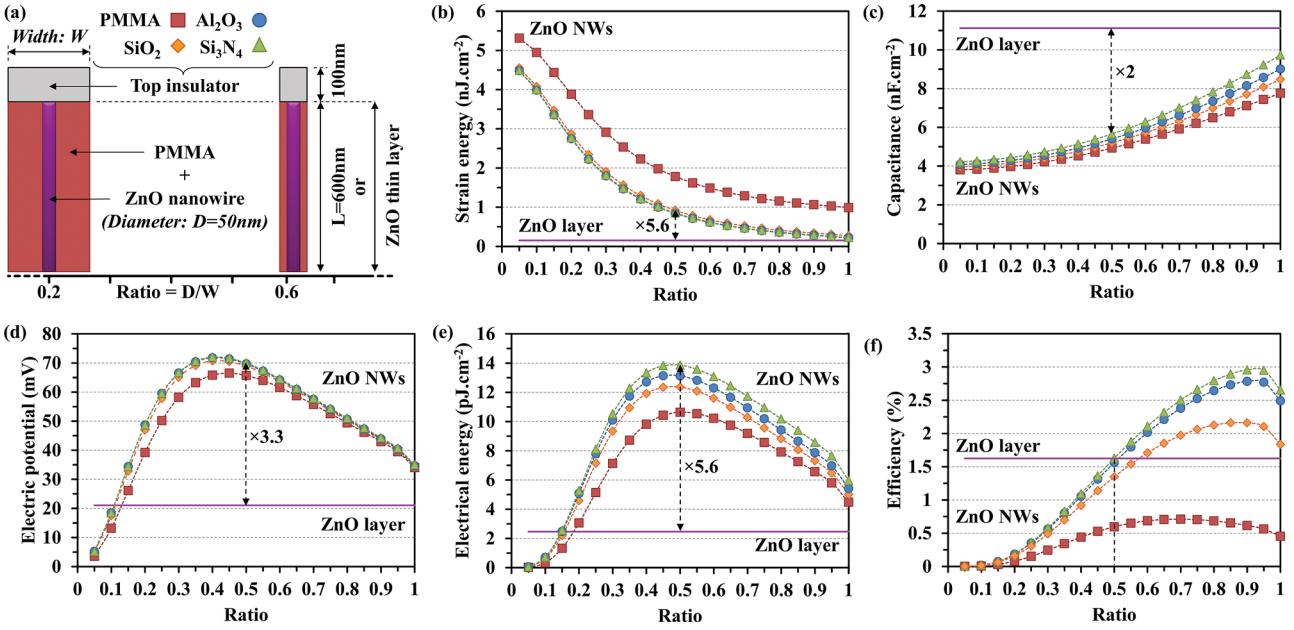

Figure 4. a) Schematics of different NG structures using various materials and NWs densities, b) mechanical energy, c) capacitance, d) electrical potential, e) electrical energy, f) efficiency of a NG core cell using different top insulating materials: PMMA, SiO_2, Al_2O_3, and Si_3N_4, function of the NWs density as the ratio parameter. The comparison with a thin ZnO layer has been done using the same FEM simulation and conditions.

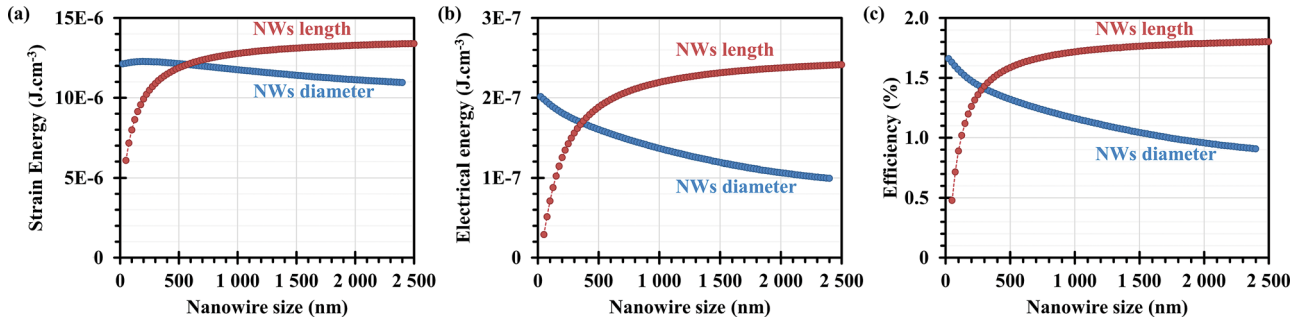

Figure 5. FEM simulation of a NG core cell using a ZnO NW embedded in PMMA with Si_3N_4 top insulator, a ratio parameter of 0.5 and under 1 MPa. a) Mechanical energy, b) electrical energy, c) efficiency as a function of NW diameter at constant length $L = 600$ nm and as a function of NW length at constant radius $r = 25$ nm.

of the NG core cell as a function of NW density. A ratio $R = 1$ corresponds to a high NW density of 4×1010 cm^{-2} and $R = 0.1$ to a low density of 4×10^8 cm^{-2}. As expected, the lower the NWs density, the higher was the mechanical energy stored in the device for a given pressure (Figure 4b). This is due to the fact that the Young's modulus is much lower in PMMA than in ZnO. With a smaller NW density, the proportion of ZnO decreases compared to PMMA, resulting in a smaller equivalent Young's modulus of the NWs layer. In the same way the capacitance is smaller (Figure 4c) due to the small permittivity of PMMA. Because of the 3D dielectric losses and the deviation of the strain field around the NWs, a soft NW layer cannot generate maximum electric potential (Figure 4d) and electrical energy (Figure 4e). As a result, a smaller NW density improved the storage of mechanical energy to the NG but reduced the electrical energy stored. In contrast, a high NW density increased the capacity to store electrical energy in the NG, at the expense of reduced mechanical energy storage. As a result, NG efficiency goes through a maximum that resultes from a trade-off between the two mechanisms (Figure 4f).

Simulations show that the maximum of electrical energy produced by a NG under a given pressure of 1 MPa was 14 pJ cm^{-2} and is achieved for an average NW density $R = 0.45$. In this study different materials were tested and the maximum electrical energy peak varied only from $R = 0.45$ to $R = 0.5$ depending on their Young modulus and permittivity. A very low NW density can be considered as equivalent to one ZnO NW with the mechanical properties of PMMA, leading to a very low energy stored. On the contrary, a high ZnO NW density will correspond to a thin layer made of a material close to ZnO. In this case it is interesting to note that the efficiency of the piezoelectric mechanical energy harvester is close to the maximum but the output electrical energy is not, because of the low force sensitivity. Now for energy harvesting applications it is better to maximize the output electrical energy than the energy harvesting efficiency. Finally to evaluate the true advantage of the new structure, we simulated the electric potential generated by a NG constituted of a thin ZnO layer with the same thickness (600 nm) and properties as the ZnO NWs. Under the same conditions, the ZnO NWs device generates an electric potential 3.3 times higher and a capacitance 2 times smaller than the ZnO layer device. Thus the generated electrical energy is 5.6 times higher due to the square of the voltage in the electric energy Equation 7, and the efficiency is almost the same at $R = 0.5$.

$$\text{Electrical energy} = \frac{1}{2} C U^2 \quad (7)$$

This improvement of the output electrical energy while maintaining the same efficiency makes the NWs based NG more sensitive to small forces. It will generate an electrical energy equivalent to a thin ZnO layer but for a smaller applied force.

The new structures were then simulated to take full advantage of a smart combination of mechanical property of PMMA, electromechanical property of Si_3N_4 and piezoelectric property of ZnO. The core layer of the device was a NWs based structure acting as a piezoelectric composite material layer.[49] We then investigated the effect of NWs size on device performances. For a given NWs length of $L = 600$ nm, we increased the diameter (D) from 24 nm to 2400 nm corresponding to a decrease of the NW aspect ratio from 25 to 0.25. The decrease in NW aspect ratio reduces the density of mechanical energy stored and the electrical energy generated (**Figure 5**a,b) which both converged toward the values for a thin ZnO layer. Efficiency also decreased (Figure 5c).

On the other hand, for a given radius of 50 nm, we increased the NW length from 600 nm to 2500 nm with a NW aspect ratio changing from 12 to 50. As a result the density of electrical energy generated and the efficiency increased up to a maximum of 241 nJ cm^{-3} (equal to 500 nW cm^{-3} at 1 Hz) and 1.8% respectively. This maximum corresponds to a nano composite material taking benefits of both mechanical properties of PMMA and piezoelectric properties of ZnO. Such a piezo ZnO NWs layer embedded in PMMA is very similar to fiber based composite materials: in our case PMMA plays the role of the matrix material which is soft and sensitive to external strain while ZnO NWs plays the role of the reinforcement material while piezoelectric properties convert the energy. Such piezo fibers are interesting for mechanical energy harvesting applications. But they are more complex because of the mix of the electro mechanical and piezoelectric properties as well as for polarity issues. The resulting optimized structure consisted of thin and long piezo NWs with an adequate density ($R = 0.5$). In addition it is important to use a hard high k top insulating material. The design could be even better using a medium NW density and a zigzag top electrode[35] around each NW. The surface capacitance calculated for such a structure was increased by 2.8% and so was the electrical energy harvested.

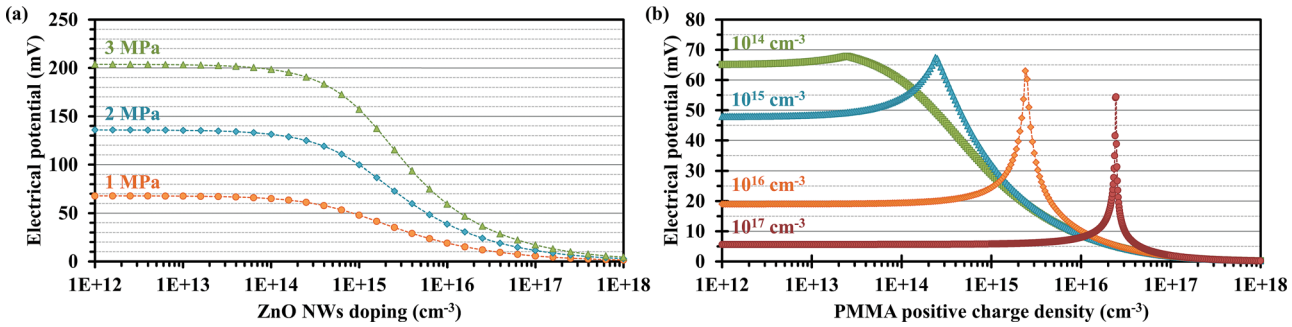

Figure 6. Piezoelectric and electrostatic FEM simulation of a NG core cell using a ZnO NW embedded in PMMA with Si_3N_4 top insulator and a ratio parameter of 0.5. a) Difference of electric potential generated under various given pressure, function of the n type doping concentration of the ZnO NW. b) Difference of electric potential generated under 1 MPa for various doping concentration of the ZnO NW, function of the positive charge density of the PMMA layer.

Besides the improvement of the electromechanical structure of the NG, ZnO semiconducting properties can also be improved. Semiconducting properties can be exploited to design ZnO NWs sensors,[50] but combination of a space charge due to ionized dopant atoms and free carriers can decrease the piezoelectric potential generated by ZnO NWs because of screening. This could be an issue for energy harvesters as previous studies have reported doping concentrations above 10^{16} to 10^{17} cm^{-3} in ZnO NWs grown by hydrothermal chemical process.[36,45] Hopefully, semiconductor structures tend to be mostly depleted at nanoscale.[51] Therefore, we simulated the influence of doping concentration on a ZnO NW using a fixed charge density. As previously, we kept the bulk values for the piezoelectric coefficients. It was found that electric potential decreased from 68 mV to 1.4 mV as doping level increased, thus reducing dramatically NG performances (**Figure 6**a).

A similar effect also occurred using charged insulating layers.[43] However, studies[18] reported an increase of the piezoelectric coefficient of ZnO NWs at nano scale by a factor close to 2 experimentally, which increased the piezo potential from 70 mV to 123 mV, electrical energy from 13.9 pJ cm^{-2} to 42.5 pJ cm^{-2} (i.e., 398 nW cm^{-3} to 1214 nW cm^{-3} at 1 Hz) and efficiency from 1.63% to 5.58%. These effects probably compensate part of the screening effect in NWs and allow NG to reach reasonable output voltage.[42] Nevertheless, by decreasing the quantity of free carriers and doping concentration in the NWs, it should be possible to decrease screening and thus increase NG output voltage. Two strategies can be foreseen: firstly, we can decrease the number of free carriers generated in the NW by improving its quality. Thus develop better growing technique is a key point. O_2 plasma or subsequent annealing process are also efficient on ZnO NWs[36] to cure the mechanical defects and oxygen vacancies which increase the number of free carriers and degrade ZnO NWs quality. Secondly, we can neutralize the charges in the NW using P–N junctions and depletion layers. Thus, using a p-type soft polymer like P_3HT instead of PMMA[41] between the NWs, it should be possible to cancel the screening effect from electrons in n-type ZnO NWs by depleting it from its free carries. When the quantity of n and p charges are equal, the potential reaches a maximum corresponding to the potential generated by a perfect depleted ZnO NW. However too many positive charges will still screen the potential. Figure 6b shows that the maximum peak of potential is very sharp and the main difficulty is to experimentally adjust the quantity of positive charges in the interstitial polymer to the quantity of n-type charges in the NWs to maximize the piezo potential. In addition, the maximum peak is narrower and more difficult to find as the n-type doping concentration of the NW gets higher. This solution is thus experimentally difficult to use and technologically challenging.

3. Conclusion

In summary, we demonstrated the electromechanical optimization of the VING structure. We investigated various materials and geometries, and we proposed an innovative and efficient NG design. The piezoelectric NWs layer was found to be equivalent to a piezoelectric composite material layer with an optimum for long and thin NWs. The comparison between the optimized ZnO NWs based NG and a thin ZnO layer based NG under the same conditions proved the viability and the interest of using NWs based NG for mechanical energy harvesting applications. If we consider only the electromechanical nanostructure, the electrical energy harvested by NG can be multiplied by a factor of 6, keeping the same efficiency as a thin piezoelectric layer and increasing the force sensitivity. This analysis can be extended to other piezoelectric materials such as GaN, PZT and $BaTiO_3$. As for semiconductor piezoelectric NWs, the screening was found to strongly limit performance, even under the assumption of full depletion, due to the space charge of ionized dopants. This degradation can only be partly compensated by the increase of piezoelectric coefficients which is expected at nanoscale.[18] Although they are difficult to grow, undoped piezoelectric NWs seem the best option. Two strategies can be used to counter screening effects: improve NWs quality using plasma and annealing[36] or deplete the NWs using positive charged matrix material. As a whole we evaluated an innovative approach of a composite piezoelectric layer mixing piezo NWs and a matrix polymer which is promising for mechanical energy harvesting applications.

Supporting Information

Supporting Information is available from the Wiley Online Library or from the author.

Acknowledgements

This work has been partly supported by the European Union 7th Framework Program, within the Network of Excellence NanoFunction under grant agreement FP7/ICT/NoE no 257375. R.H. received partial support from UJF Grenoble (Smingue) and the Rhône-Alpes region.

Received: June 25, 2013
Revised: August 4, 2013
Published online: October 8, 2013

[1] Z. L. Wang, *Adv. Funct. Mater.* **2008**, *18*, 3553.
[2] M. S. Dresselhaus, I. L. Thomas, *Nature* **2001**, *414*, 332.
[3] A. I. Boukai, Y. Bunimovich, J. Tahir-Kheli, J.-K. Yu, W. A. Goddard, J. R. Heath, *Nature* **2008**, *451*, 168.
[4] A. I. Hochbaum, P. Yang, *Chem. Rev.* **2010**, *110*, 527.
[5] B. Tian, X. Zheng, T. J. Kempa, Y. Fang, N. Yu, G. Yu, J. Huang, C. M. Lieber, *Nature* **2007**, *449*, 885.
[6] N. S. Lewis, *Science* **2007**, *315*, 798.
[7] J. F. Wishart, *Energy Environ. Sci.* **2009**, *2*, 956.
[8] R. Zhang, L. Lin, Q. Jing, W. Wu, Y. Zhang, Z. Jiao, L. Yan, R. P. S. Han, Z. L. Wang, *Energy Environ. Sci.* **2012**, *5*, 8528.
[9] Z. Li, G. Zhu, R. Yang, A. C. Wang, Z. L. Wang, *Adv. Mater.* **2010**, *22*, 2534.
[10] Y. Hu, Y. Zhang, C. Xu, L. Lin, R. L. Snyder, Z. L. Wang, *Nano Lett.* **2011**, *11*, 2572.
[11] Z. L. Wang, J. Song, *Science* **2006**, *312*, 242.
[12] J. Zhou, Y. Gu, P. Fei, W. Mai, Y. Gao, R. Yang, G. Bao, Z. L. Wang, *Nano Lett.* **2008**, *8*, 3035.
[13] T. D. Nguyen, J. M. Nagarah, Y. Qi, S. S. Nonnenmann, A. V. Morozov, S. Li, C. B. Arnold, M. C. McAlpine, *Nano Lett.* **2010**, *10*, 4595.
[14] J. Wang, M. S. Gudiksen, X. Duan, Y. Cui, C. M. Lieber, *Science* **2001**, *293*, 1455.
[15] F. Patolsky, G. Zheng, C. M. Lieber, *Anal. Chem.* **2006**, *78*, 4260.
[16] A. K. Wanekaya, W. Chen, N. V. Myung, A. Mulchandani, *Electroanalysis* **2006**, *18*, 533.
[17] Q. Wan, Q. H. Li, Y. J. Chen, T. H. Wang, X. L. He, J. P. Li, C. L. Lin, *Appl. Phys. Lett.* **2004**, *84*, 3654.
[18] H. D. Espinosa, R. A. Bernal, M. Minary-Jolandan, *Adv. Mater.* **2012**, *24*, 4656.
[19] Z. L. Wang, *J. Phys. Chem. Lett.* **2010**, *1*, 1388.
[20] C.-T. Huang, J. Song, W.-F. Lee, Y. Ding, Z. Gao, Y. Hao, L.-J. Chen, Z. L. Wang, *J. Am. Chem. Soc.* **2010**, *132*, 4766.
[21] C.-Y. Chen, G. Zhu, Y. Hu, J.-W. Yu, J. Song, K.-Y. Cheng, L.-H. Peng, L.-J. Chou, Z. L. Wang, *ACS Nano* **2012**, *6*, 5687.
[22] L. Gu, N. Cui, L. Cheng, Q. Xu, S. Bai, M. Yuan, W. Wu, J. Liu, Y. Zhao, F. Ma, Y. Qin, Z. L. Wang, *Nano Lett.* **2013**, *13*, 91.
[23] Y. Qi, J. Kim, T. D. Nguyen, B. Lisko, P. K. Purohit, M. C. McAlpine, *Nano Lett.* **2011**, *11*, 1331.
[24] K.-I. Park, S. Xu, Y. Liu, G.-T. Hwang, S.-J. L. Kang, Z. L. Wang, K. J. Lee, *Nano Lett.* **2010**, *10*, 4939.
[25] Z.-H. Lin, Y. Yang, J. M. Wu, Y. Liu, F. Zhang, Z. L. Wang, *J. Phys. Chem. Lett.* **2012**, *3*, 3599.
[26] J. H. Jung, M. Lee, J.-I. Hong, Y. Ding, C.-Y. Chen, L.-J. Chou, Z. L. Wang, *ACS Nano* **2011**, *5*, 10041.
[27] C. Chang, V. H. Tran, J. Wang, Y.-K. Fuh, L. Lin, *Nano Lett.* **2010**, *10*, 726.
[28] C. Xu, C. Pan, Y. Liu, Z. L. Wang, *Nano Energy* **2012**, *1*, 259.
[29] X. Chen, S. Xu, N. Yao, Y. Shi, *Nano Lett.* **2010**, *10*, 2133.
[30] R. Yang, Y. Qin, L. Dai, Z. L. Wang, *Nat. Nanotechnol.* **2009**, *4*, 34.
[31] S. Xu, Y. Qin, C. Xu, Y. Wei, R. Yang, Z. L. Wang, *Nat. Nanotechnol.* **2010**, *5*, 366.
[32] Y. Qi, N. T. Jafferis, K. Lyons, C. M. Lee, H. Ahmad, M. C. McAlpine, *Nano Lett.* **2010**, *10*, 524.
[33] Y. Qin, X. Wang, Z. L. Wang, *Nature* **2008**, *451*, 809.
[34] M. Lee, C.-Y. Chen, S. Wang, S. N. Cha, Y. J. Y. J. Park, J. M. Kim, L.-J. Chou, Z. L. Wang, *Adv. Mater.* **2012**, *24*, 1759.
[35] X. Wang, J. Song, J. Liu, Z. L. Wang, *Science* **2007**, *316*, 102.
[36] Y. Hu, L. Lin, Y. Zhang, Z. L. Wang, *Adv. Mater.* **2012**, *24*, 110.
[37] S. Lee, J.-I. Hong, C. Xu, M. Lee, D. Kim, L. Lin, W. Hwang, Z. L. Wang, *Adv. Mater.* **2012**, *24*, 4398.
[38] S. Lee, S.-H. Bae, L. Lin, Y. Yang, C. Park, S.-W. Kim, S. N. Cha, H. Kim, Y. J. Park, Z. L. Wang, *Adv. Funct. Mater.* **2013**, *23*, 2445.
[39] J. I. Sohn, S. N. Cha, B. G. Song, S. Lee, S. M. Kim, J. Ku, H. J. Kim, Y. J. Park, B. L. Choi, Z. L. Wang, J. M. Kim, K. Kim, *Energy Environ. Sci.* **2013**, *6*, 97.
[40] O. Graton, G. Poulin-Vittrant, L. Hue, M. Lethiecq, in *PowerMEMS 2010*, Transducer Research Foundation, San DiegoUS[[**2010**, p 391.
[41] K. Y. Lee, B. Kumar, J.-S. Seo, K.-H. Kim, J. I. Sohn, S. N. Cha, D. Choi, Z. L. Wang, S.-W. Kim, *Nano Lett.* **2012**, *12*, 1959.
[42] G. Zhu, A. C. Wang, Y. Liu, Y. Zhou, Z. L. Wang, *Nano Lett.* **2012**, *12*, 3086.
[43] S. Lee, R. Hinchet, Y. Lee, Y. Yang, Z.-H. Lin, G. Ardila, L. Montès, M. Mouis, Z. L. Wang, *Adv. Funct. Mater.* **2013**, DOI: 10.1002/adfm.201301971.
[44] Z. L. Wang, *Adv. Mater.* **2012**, *24*, 280.
[45] S. Xu, C. Xu, Y. Liu, Y. Hu, R. Yang, Q. Yang, J.-H. Ryou, H. J. Kim, Z. Lochner, S. Choi, R. Dupuis, Z. L. Wang, *Adv. Mater.* **2010**, *22*, 4749.
[46] COMSOL Multiphysics simulation software, http://www.comsol.com (accessed September, **2013**).
[47] Y. Gao, Z. L. Wang, *Nano Lett.* **2007**, *7*, 2499.
[48] R. Hinchet, S. Lee, G. Ardila, L. Montes, M. Mouis, Z. L. Wang, in *PowerMEMS 2012*, Transducer Research Foundation, San Diego, US **2012**.
[49] S. Xu, Y. Yeh, G. Poirier, M. C. McAlpine, R. A. Register, N. Yao, *Nano Lett.* **2013**, *13*, 2393.
[50] R. Hinchet, J. Ferreira, J. Keraudy, G. Ardila, E. Pauliac-Vaujour, M. Mouis, L. Montes, in *2012 International Electron Devices Meeting*, IEEE, Piscataway, US **2012**, p 119.
[51] B. S. Simpkins, M. A. Mastro, C. R. Eddy, P. E. Pehrsson, *J. Appl. Phys.* **2008**, *103*, 104313.